16th World Conference on Earthquake, 16WCEE 2017
Santiago Chile, January 9th to 13th 2017
Paper N° 0425
Registration Code: S-W1461634130

MECHANICAL CHARACTERISTICS OF ADAPTIVE RUBBER BEARINGS

C. S. Tsai [1], H. C. Su [2], W. C. Huang [3] , T. C. Chiang [4]

[1] Distinguished Professor, Department of Civil Engineering, Feng Chia University, Taichung, Taiwan, cstsai@mail.fcu.edu.tw
[2] Associate Professor, Department of Water Resources Engineering and Conservation, Feng Chia University, Taichung, Taiwan, hcsu@fcu.edu.tw
[3] Master Student, Department of Civil Engineering, Feng Chia University, Taichung, Taiwan, outside369842@yahoo.com.tw
[4] Technical Manager, Earthquake Proof Systems, Inc., Taichung, Taiwan, rickchiang19771011@gmail.com

Abstract

Proposed in this study are several innovative seismic isolators consisting of rubber materials that are called adaptive rubber bearings because of their adaptive characteristics. The materials used in the proposed isolators are free of lead which is commonly found in lead rubber bearings. The lead material results in heavy environmental burden and lower yield strength and damping due to rising temperature during earthquakes, causing larger displacements than we would expect. The designed mechanisms in the proposed isolators enable these devices relatively easily manufactured and also provide extremely high damping to the bearings, which is highly desired by engineers in practice. The proposed rubber bearings are completely passive devices yet possess adaptive stiffness and damping. The change in stiffness and damping is predicable and can be calculated at specifiable and controllable displacement amplitudes. The major benefit of the adaptive characteristic of seismic isolators is that a given system can be optimized separately for multiple performance objects at multiple levels of earthquakes. In this paper, mathematical formulations have been derived to explain the mechanisms of the proposed devices. Experimental results are also provided to verify the advanced concept of the proposed devices.

Keywords: seismic isolation; rubber bearing; base isolator; adaptive rubber bearing; high damping rubber bearing

1. Introduction

Base isolation technology that lessens the seismic responses of a structure by inserting a flexible connection between the structure and the ground, which is necessary to transfer the natural period of a structure from the predominant period of the ground, has been recognized worldwide as a promising technique to protect existing and new structures from earthquake damage. This has been verified through extensive experimental and numerical studies as well as field measurements taken during earthquakes. Among the techniques [1-4] achieving a flexible connection and having gained acceptance, three types of popular seismic isolation systems have been proven to reduce the seismic responses of structures and equipments efficiently. These are the elastomeric bearing-based [5-7], sliding-based [8-16], and rolling systems [3, 4]. In 1869, the American L. Sterne [3, 17], stated concerning his invention as shown in Fig. 1: "My invention consists of a novel construction of spring, more particularly applicable to or as buffers, bearing and drawing springs for railway purposes, which is of the character of a pneumatic rubber spring, and is made or built up of soft India-rubber rings, and circular or other suitable shaped metal-plates, the rubber rings being chemically united to the plates during the process of vulcanization, and being alternately arranged in relation to said plates, ..." This device was proposed as a bearing for railway purposes. It was not intended as a means for seismic isolation. However, it already represented an embryonic form of chemically uniting alternately arranged plates and rubber layers during the process of vulcanization and curing. It could function as a modern seismic isolator. In 1978, W. H. Robinson of New Zealand [7] increased the damping ratio of the device by inserting a lead core into the center of the system proposed by Sterne that included alternately layered rubbers and steel plates. Robinson's lead rubber bearing (LRB) could be, if made up-to-date, the most popular rubber bearing for use in engineering applications in the world. However, the lead material used in a LRB results in heavy environmental burden as well as lower yield

strength and damping resulting from rising temperatures during earthquakes. The lower damping causes larger displacements than we would expect.

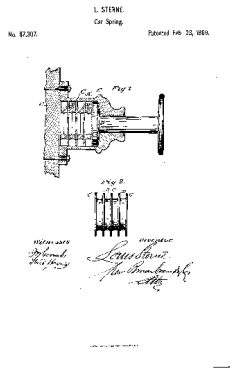

Fig. 1 – L. Sterne's original patent (1869**)**

In this study, several new types of seismic isolators composed of rubber materials and called adaptive rubber bearings (ARBs) are proposed to solve the aforementioned problems encountered by LRBs. These isolators use nature-friendly materials and are free of lead. The proposed rubber bearings are completely passive, yet possess adaptive characteristics of stiffness and damping. Their change in stiffness and damping is predictable and can be calculated at controllable displacement amplitudes. In addition to achieving adaptive behavior, the proposed rubber bearings possess an extremely high damping ratio of approximately 60% at small displacements according to experimental results (referred to Section 4) to improve the performance of a structure in terms of acceleration response and isolator deformation if low frequency is dominant in the ground motion, as well as achieve medium to high damping ratios for ground motion with dominant high frequency content by adopting different sizes or materials of sliding plates at individual layers (experimental results are not presented in this paper due to the page limit). Therefore, the damping ratio of the ARB is adjustable and dependent on the demands of engineering, which is desired by engineers in practice. In this study, mathematical formulations are derived to explain the mechanism of the proposed bearings. In addition, experimental results are provided to verify the concept proposed devices. The proposed isolators have the following advantages when compared to the LRB: (1) uses environmentally friendly materials, (2) has fewer temperature rising problems, (3) distributes uniform force without stress concentration at specific areas of the energy absorption core, (4) has much higher damping, (5) possesses adaptive characteristics, (6) is easier to manufacture, (7) is lighter, (8) allows for the deformation of rubber layers to be optimized individually for multiple performance objects at multiple levels of earthquakes, and (9) has independently adjustable vertical stiffness obtained from combinations of various materials of sliding plates without coupling with the horizontal stiffness provided by rubber.

2. Major Concepts of Proposed Rubber Bearings

An LRB adopts the heavy metal of lead to absorb vibration energy by yielding the lead material that produces a major burden on the environment. The yield point of the lead material is a function of ambient temperature and rising temperature from heat derived from absorbed seismic energy. To solve the aforementioned problems encountered by the LRB, a series of innovative seismic isolators have been proposed [18, 19]. The major concepts behind the proposed isolators are described as follows. As shown in Fig. 2, the seismic isolator consists of alternate rubber layers and shim plates that act as traditional rubber bearings. However, the major contribution of the proposed device is the new sliding core, which includes multiple sliding plates used at each rubber layer to produce multiple sliding surfaces that are located between and confined by two adjacent shim plates. This aids in leveling the arrangements of shim plates and rubber materials during manufacturing processes. These sliding plates also distribute the displacement of a single rubber layer into multiple sliding interfaces and smooth the sliding motion during earthquakes. This leads to a smaller displacement and reduces the amount of heat derived from the friction of the sliding motion on each sliding plate of a single layer. The friction coefficient can be different from one sliding interface or rubber layer to another, which is necessary to control the time required to

initiate the sliding motion of a sliding plate or rubber layer. No deformation occurs in a rubber layer during sliding motion on the sliding surface if the horizontal force is less than the frictional force at any sliding interface of that layer. When the horizontal force overcomes the frictional force of the interface in a specific layer, the layer is subjected to shear deformation. In addition, a sliding motion occurs on the interface of two adjacent sliding plates to provide damping as a result of the frictional force on this sliding interface. The multiple sliding plates are confined between two adjacent shim plates to smooth the sliding motion and achieve adaptive functions based on the design of friction coefficients of these sliding interfaces. The sliding surfaces of each layer of the sliding core provide the device with adaptive functions and produce high damping effects. This is accomplished by controlling the deformation contribution of the rubber layer based on the predesigned frictional force on each sliding surface. No deformation or sliding motion will occur at a specific rubber layer if the horizontal force of the device is smaller than the frictional force of a sliding interface in that particular layer. The layer will not induce damping in the system. In addition, the stiffness of the particular layer will be infinite. Any one of the sliding interfaces in a specific rubber layer will be activated and begin sliding to produce damping if the horizontal force is greater than the frictional force of this particular sliding interface of this layer. Simultaneously, the rubber within the activated sliding plate in this activated layer will begin to deform, which will contribute to damping and flexibility or stiffness. The mechanical behavior of the entire seismic isolator is based on the series connections of activated layers. The major parameters for controlling the adaptive characteristics of the entire system are the friction coefficient and sustained vertical load at each sliding interface.

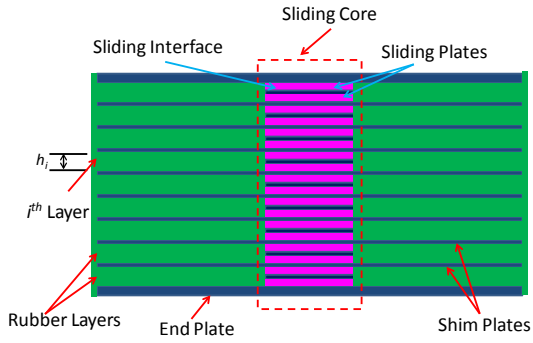

Fig. 2 – Cross sectional view of the first type of adaptive rubber bearing (3 sliding plates in each layer)

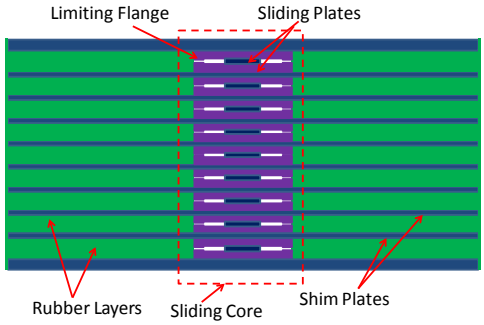

Fig. 3 – Cross sectional view of the second type of adaptive rubber bearing with three sliding plates having limiting flanges at each layer

Figures 3 and 4 show an annular limiting flange at the edge of the sliding plate. This is used to limit displacement to a predesigned value at a single layer of the second type of ARB. Figure 4 demonstrates that the lower sliding interface on Sliding Plate 2 reaches its displacement capacity in order to stop sliding motion and rubber deformation at the lower part of the i^{th} layer of the isolator. When the displacement of the sliding interface reaches this predefined value, the sliding motion of the sliding interface on this layer will stop and a certain amount of rubber thickness dominated by this sliding plate will be unable to contribute its deformation and flexibility to the layer and to the whole device. Therefore, the stiffness of the entire seismic isolator will increase, thereby reducing the isolator displacement during a massive earthquake by excluding the flexibility of this particular layer. This means that selecting proper materials for the sliding plates and setting controllable displacement limits at sliding interfaces are crucial to achieving optimum designs for multiple levels of ground motion. The damping effect of the entire system is the sum of contributions from friction that occurs at the activated sliding interfaces and the deformation of rubber layers. The stiffness of the whole device derives from the connection of series of active rubber layers provided that the horizontal force overcomes the frictional force and a layer's displacement remains within the displacement limit.

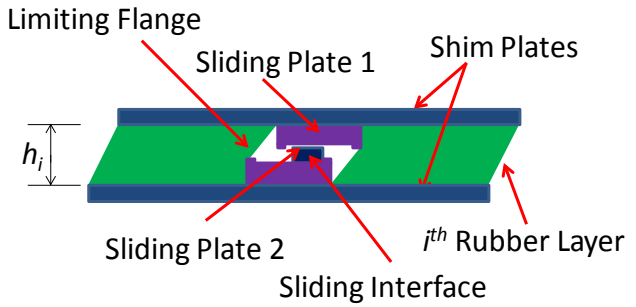

Fig. – 4 Sliding motion of sliding plates with limiting flange and rubber deformation in a single layer (two major sliding interfaces)

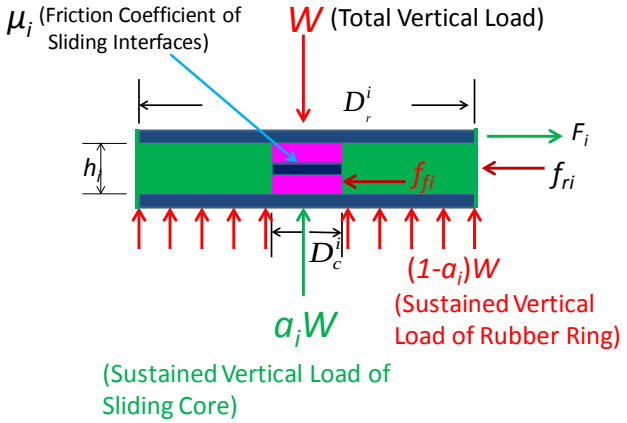

Fig. – 5 Forces in a typical single layer of isolator

In general, the adaptive functions can be achieved by adjusting the friction coefficients, predefined displacement capacities, and sizes of sliding plates such as diameter and thickness, as well as the thickness and material properties of rubber layers. These in turn adjust the vertical stiffness, sustained vertical loads, and frictional forces on the sliding plates and sliding interfaces. Many possible combinations of the aforementioned parameters can be adjusted to achieve multiple performance targets at multiple levels of earthquakes. The following facts should be noted regarding the proposed device and its features. First, the device can more easily generate different thicknesses of rubber layers because the sliding plates in each layer can provide adequate support in leveling shim plates and rubber layers during the vulcanization and curing processes. Second, the total thickness of the sliding plates at each rubber layer will be the thickness of the rubber layer. Third, the sliding plates will be helpful in sustaining vertical load as a result of their high strength and rigidity in the vertical direction. Fourth, the sliding displacement at each sliding interface is equal to the displacement at each rubber layer divided by the total number of the sliding layers at each rubber layer. Fifth, the sliding displacement of each sliding plate will be extremely small compared to its diameter or length because multiple sliding interfaces are arranged in each rubber layer to distribute sliding displacement. Finally, the absorbed seismic energy in the sliding core will be distributed to sliding interfaces without causing a significant rise in temperature because heat produced by the sliding motion at each sliding interface will be uniform and reduced. This reduced heat results from a considerably smaller sliding displacement that occurs at each sliding interface without bending occurring, unlike lead deformation in the LRB. The materials used by ARBs have much higher specific heat than that of lead material used by the LRB that is equal to 0.033.

3. Effective Stiffness and Equivalent Damping of ARB

This section describes the mathematical formulations necessary to illustrate the major concepts of the proposed isolator. Figure 5 shows the forces in a typical single layer. The rubber layer and multiple sliding plates of the sliding core in a single layer are connected in parallel. Therefore, the total horizontal force, F_i, in a single layer is the sum of the shear force of the rubber and the frictional force of the sliding plate and given by:

$$F_i = f_{ri} + f_{fi} = (k_{eff}^{ri} + k_{eff}^{fi})u_i = k_{eff}^{i} u_i \quad (1)$$

where f_{ri} denotes the shear force of the i^{th} layer of the rubber material; f_{fi} represents the frictional force of the sliding interface; u_i is the relative displacement between the top and bottom of the i^{th} layer; k_{eff}^{ri} denotes the effective stiffness of rubber material in the i^{th} layer, as shown in Fig. 6; and k_{eff}^{fi} is the effective stiffness of the sliding plate in the i^{th} layer, as shown in Fig. 7. In addition, k_{eff}^{i} is the total effective stiffness of the i^{th} layer,

which means that $k_{eff}^{i} = k_{eff}^{ri} + k_{eff}^{fi}$ and $k_{eff}^{ri} = G_r^i A_r^i / h_i$ [5], where G_r^i, h_i, and A_r^i are the shear modulus, thickness, and cross-sectional area of rubber in the i^{th} layer, respectively.

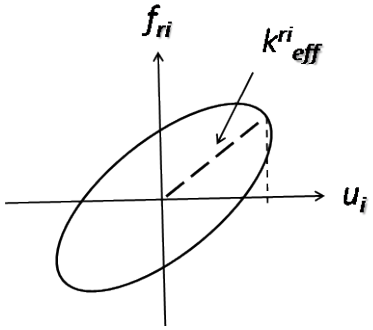

Fig. – 6 Hysteretic loop of a single layer of rubber material

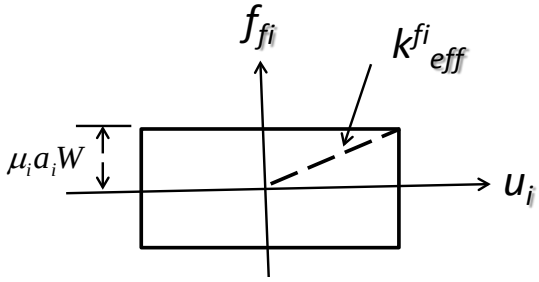

Fig. – 7 Hysteretic loop of sliding core in a single layer

The total enclosed area, A_i, of the force-displacement loop of the i^{th} layer is the sum of the rubber, A_{ri}, and the sliding plates, A_{fi}. This is given as:

$$A_i = A_{ri} + A_{fi} \tag{2}$$

As Fig. 6 shows, the enclosed area of the force-displacement loop of the sole rubber of the i^{th} layer is given by:

$$A_{ri} = 2\pi k_{eff}^{ri} u_i^2 \xi_{ri} \tag{3}$$

where ξ_{ri} is the equivalent damping ratio of the sole rubber in the i^{th} layer.

As shown in Fig. 7, the enclosed area of the force-displacement loop of sole sliding plates of the i^{th} layer is obtained as:

$$A_{fi} = 4u_i f_{fi} = 4(\mu_i a_i W)u_i \tag{4}$$

where a_i denotes a percentage of the total vertical load sustained by the sliding plates (this is derived in a later section); and W represents the total vertical load on the seismic isolator resulting from the dead load and the occurrence of an earthquake.

The effective stiffness of sliding plates of the i^{th} layer, k_{eff}^{fi}, is given by:

$$k_{eff}^{fi} = \frac{f_{fi}}{u_i} = \frac{\mu_i a_i W}{u_i} \tag{5}$$

The total effective stiffness of the i^{th} layer, which includes the rubber and sliding plates, can be expressed as:

$$k_{eff}^{i} = k_{eff}^{ri} + \frac{\mu_i a_i W}{u_i} \tag{6}$$

The total area of the isolator enclosed by the hysteretic loop of the device, A, is the sum of the areas enclosed by the active rubber layers and the friction forces of the activated sliding interfaces in the sliding core.

If the n^{th} layer is not activated, the total area is obtained by excluding the effects of the n^{th} layer by means of the following.

$$A = \sum_{\substack{i=1 \\ i\neq n}}^{N} \left(A_{ri} + A_{fi}\right) = \sum_{\substack{i=1 \\ i\neq n}}^{N} (2\pi k_{eff}^{ri} u_i^2 \xi_{ri} + 4a_i W \mu_i u_i) \tag{7}$$

where N is the total number of layers in the device.

The total horizontal force of the i^{th} layer is given by:

$$F_i = (k_{eff}^{ri} + k_{eff}^{fi}) u_i = k_{eff}^{ri} u_i + a_i W \mu_i \tag{8}$$

Rearranging Eq. (8) yields a relative displacement between the top and bottom of the i^{th} layer. We thus derive the following.

$$u_i = \frac{F_i - a_i W \mu_i}{k_{eff}^{ri}} \tag{9}$$

If the horizontal force sustained by the sliding plates is smaller than the frictional force at the n^{th} layer, $a_n W \mu_n$, the total displacement u of the isolator is equal to the sum of the displacements of all layers except for the n^{th} layer and given by:

$$u = \sum_{\substack{i=1 \\ i\neq n}}^{N} u_i = \sum_{\substack{i=1 \\ i\neq n}}^{N} \frac{F_i - a_i W \mu_i}{k_{eff}^{ri}} = F \sum_{\substack{i=1 \\ i\neq n}}^{N} \frac{1}{k_{eff}^{ri}} - \sum_{\substack{i=1 \\ i\neq n}}^{N} \frac{a_i W \mu_i}{k_{eff}^{ri}} \tag{10}$$

The total horizontal force of the entire isolator can be obtained with the aid of Eq. (10) by the following.

$$F = \frac{1}{\sum_{\substack{i=1 \\ i\neq n}}^{N} \frac{1}{k_{eff}^{ri}}} u + \frac{1}{\sum_{\substack{i=1 \\ i\neq n}}^{N} \frac{1}{k_{eff}^{ri}}} \sum_{\substack{i=1 \\ i\neq n}}^{N} \frac{a_i W \mu_i}{k_{eff}^{ri}} \tag{11}$$

If the horizontal force sustained by the sliding plate is smaller than the frictional force at the n^{th} layer, $a_n W \mu_n$, or the displacement of a particular layer reaches the predesigned displacement capacity of this layer, the total stiffness of the rubber layers of the isolator, K_{eff}^{rb}, is a result of all layers of sole rubber materials connected in a series by excluding the contribution of this particular layer, which is inactive. This is derived as:

$$\frac{1}{K_{eff}^{rb}} = \sum_{\substack{i=1 \\ i\neq n}}^{N} \frac{1}{k_{eff}^{ri}} = \frac{1}{k_{eff}^{r1}} + \frac{1}{k_{eff}^{r2}} + \frac{1}{k_{eff}^{r3}} + ... + \frac{1}{k_{eff}^{rn-1}} + \frac{1}{k_{eff}^{rn+1}} .. + \frac{1}{k_{eff}^{rN}} \tag{12}$$

The total horizontal stiffness of all layers of sole rubber materials, K_{eff}^{rb}, in the whole device, excluding the contribution from the n^{th} layer, can be expressed with the aid of Eq. (12) as:

$$K_{eff}^{rb} = \frac{k_{eff}^{r1} k_{eff}^{r2} k_{eff}^{r3} ... k_{eff}^{rn-1} k_{eff}^{rn+1} ..... k_{eff}^{rN-1} k_{eff}^{rN}}{k_{eff}^{r2} k_{eff}^{r3} .... k_{eff}^{rn-1} k_{eff}^{rn+1} .... k_{eff}^{rN} + ... + k_{eff}^{r1} k_{eff}^{r2} k_{eff}^{r3} .. k_{eff}^{rn-1} k_{eff}^{rn+1} ..... k_{eff}^{rN-1}} \tag{13}$$

Substituting (13) with (11) leads to:

$$F = K_{eff}^{rb} u + K_{eff}^{rb} \sum_{\substack{i=1 \\ i \neq n}}^{N} \frac{a_i W \mu_i}{k_{eff}^{ri}} = K_{eff}^{rb} u + F_{eff}^{f} \tag{14}$$

where the equivalent frictional force of the entire system, F_{eff}^{f}, is given by:

$$F_{eff}^{f} = K_{eff}^{rb} \sum_{\substack{i=1 \\ i \neq n}}^{N} \frac{a_i W \mu_i}{k_{eff}^{ri}} \tag{15}$$

The relative displacement between the top and bottom of the i^{th} layer can be obtained by substituting Eq. (14) with Eq. (9) to arrive at:

$$u_i = \frac{F_i - a_i W \mu_i}{k_{eff}^{ri}} = \frac{F - a_i W \mu_i}{k_{eff}^{ri}} = \frac{1}{k_{eff}^{ri}} \left[\left(K_{eff}^{rb} u + K_{eff}^{rb} \sum_{\substack{i=1 \\ i \neq n}}^{N} \frac{a_i W \mu_i}{k_{eff}^{ri}} \right) - a_i W \mu_i \right] \tag{16}$$

Substituting Eq. (16) with Eq. (4) results in an enclosed area of the force-displacement loop of the sliding interfaces in the i^{th} layer such that:

$$A_{fi} = 4(\mu_i a_i W) u_i = \frac{4 \mu_i a_i W}{k_{eff}^{ri}} \left[\left(K_{eff}^{rb} u + K_{eff}^{rb} \sum_{\substack{i=1 \\ i \neq n}}^{N} \frac{a_i W \mu_i}{k_{eff}^{ri}} \right) - a_i W \mu_i \right] \tag{17}$$

The enclosed area of the force-displacement of the sole rubber of the i^{th} layer can be obtained with the aid of Eqs. (16) and (3) to arrive at:

$$A_{ri} = \frac{2 \pi \xi_{ri}}{k_{eff}^{ri}} \left[\left(K_{eff}^{rb} u + K_{eff}^{rb} \sum_{\substack{i=1 \\ i \neq n}}^{N} \frac{a_i W \mu_i}{k_{eff}^{ri}} \right) - a_i W \mu_i \right]^2 \tag{18}$$

Substituting Eqs. (17) and (18) with Eq. (7) leads to the equivalent damping ratio of the entire isolator provided that the n^{th} layer is not active. This yields:

$$\xi_e = \frac{1}{2 \pi K_{eff} u^2} \sum_{\substack{i=1 \\ i \neq n}}^{N} \left(A_{ri} + A_{fi} \right) = \frac{1}{2 \pi K_{eff} u^2} \left\{ \sum_{\substack{i=1 \\ i \neq n}}^{N} \frac{2 \pi \xi_{ri}}{k_{eff}^{ri}} \left[\left(K_{eff}^{rb} u + K_{eff}^{rb} \sum_{\substack{i=1 \\ i \neq n}}^{N} \frac{a_i W \mu_i}{k_{eff}^{ri}} \right) - a_i W \mu_i \right]^2 \right\} \tag{19}$$

$$+ \frac{1}{2 \pi K_{eff} u^2} \left\{ \sum_{\substack{i=1 \\ i \neq n}}^{N} \frac{4 \mu_i a_i W}{k_{eff}^{ri}} \left[\left(K_{eff}^{rb} u + K_{eff}^{rb} \sum_{\substack{i=1 \\ i \neq n}}^{N} \frac{a_i W \mu_i}{k_{eff}^{ri}} \right) - a_i W \mu_i \right] \right\}$$

The vertical stiffness of the sole rubber in the i^{th} layer is given by the following [5].

$$k_{rV}^{i} = \frac{E_r^i A_{rubber}^i}{h_i} \tag{20}$$

where

$$E_r^i = 6G_r^i S^2 \lambda \tag{21}$$

Here, S denotes the shape factor of the i^{th} layer of rubber and is equal to $\left(D_r^i - D_c^i\right)/4h_i$ for a circular cross section. In addition, λ is a parameter of the rubber layer to define the vertical stiffness of rubber and is given by [5]:

$$\lambda = \frac{1}{(1-D_c^i/D_r^i)^2}\left[1+(D_c^i/D_r^i)^2 + \frac{1-(D_c^i/D_r^i)^2}{\ln(D_c^i/D_r^i)}\right] \tag{22}$$

where D_r^i and D_c^i are the diameters of the rubber layer and sliding core of the i^{th} layer of the isolator, respectively, as shown in Fig. 5.

The sliding plates in a single layer are connected in a series to yield the vertical stiffness of the i^{th} layer of the sliding core as:

$$k_{fV}^i = \frac{k_{fV}^{f1}k_{fV}^{f2}k_{fV}^{f3}\ldots k_{fV}^{fM-1}k_{fV}^{fM}}{k_{fV}^{f2}k_{fV}^{f3}\ldots k_{fV}^{fM} + \ldots + k_{fV}^{f1}k_{fV}^{f2}k_{fV}^{f3}\ldots k_{fV}^{fM-1}} \tag{23}$$

where M is the total number of sliding plates in the i^{th} layer (a single layer with multiple sliding plates) and k_{fV}^{fj} is the vertical stiffness of the j^{th} sliding plate in the i^{th} layer of the sliding core.

The ratio of the vertical stiffness of sliding plates in a single layer to that of the total vertical stiffness of the i^{th} layer, which is the percentage of the total vertical load to be sustained by the sliding plates in a single layer, can be obtained as:

$$a_i = \frac{k_{fV}^i}{k_{rV}^i + k_{fV}^i} \tag{24}$$

The total vertical stiffness of the i^{th} layer, k_V^i, is the sum of the vertical stiffness of rubber and sliding plates, given as:

$$k_V^i = k_{rV}^i + k_{fV}^i \tag{25}$$

The total vertical stiffness of the entire isolator is obtained by connecting all layers in a series using:

$$K_V = \frac{k_V^1 k_V^2 k_V^3 \ldots k_V^{N-1}k_V^N}{k_V^2 k_V^3 \ldots k_V^N + \ldots + k_V^1 k_V^2 k_V^3 \ldots k_V^{N-1}} \tag{26}$$

In the case of identical material properties including those of rubbers and sliding plates in all layers, we have $a=a_i$ and $\mu = \mu_i$ to yield the following [19].

$$\xi_e = \frac{\xi_e^{rb}}{1+\frac{aW\mu}{K_{eff}^{rb}u}} + \frac{2}{\pi}\frac{1}{1+\frac{K_{eff}^{rb}u}{aW\mu}} \tag{27}$$

where a_i is the percentage of the total vertical load to be sustained by the sliding core.

The effective stiffness of the entire isolator, which combines rubber layers and the sliding core, is obtained by:

$$K_{eff} = K_{eff}^{rb} + \frac{aW\mu}{u} \tag{28}$$

As seen in Eq. (27), the equivalent damping ratio of the entire system approaches 63.7% whereas the displacement is approximately equal to zero. In addition, the equivalent damping ratio of the device approaches that of the sole rubber layers of the whole isolator if the displacement becomes extremely large. This is one of the advantages of this device, which provides a great value of damping ratio resulting from the sliding motion of sliding interfaces in the sliding core. The major parameters from Eq. (27) that influence the equivalent damping ratio of the entire isolation system are the following: the effective stiffness of all layers of rubber, sustained vertical loading of the sliding core, friction coefficients of sliding interfaces, equivalent damping ratio of rubber layers, and isolator displacement. The more the sustained vertical loading of the sliding core and friction coefficients of sliding interfaces are, the higher is the equivalent damping ratio. The reduced stiffness of sole rubber layers will increase the equivalent damping ratio of the isolator. The greater is the displacement, the smaller is the contribution from sliding motion and the larger is the contribution from rubbers to the equivalent damping ratio. The derived Eq. (27) reveals that softer rubber material, a higher friction coefficient, and greater vertical stiffness of the sliding core results in a higher damping ratio. If no damping ratio for rubber exists, if the effective horizontal stiffness is equal to *W/R*, such as in a friction pendulum system, and if all vertical load is sustained by sliding plates, then the equivalent damping ratio of the entire isolator will be $\xi_e = (2/\pi)[\mu_i/(\mu_i + u/R)]$. This is identical to the equivalent damping ratio of a single friction pendulum system or a multiple pendulum system, where *R* is the radius of the sliding concave surface of the single friction pendulum system [8, 10-13].

4. Experimental Results and Discussion

In this section, test results of scaled ARB specimens are presented to verify the concept proposed in this study. As shown in Fig. 8, the tested bearing of the first type was 140 mm in diameter, and had a 3-mm cover, a sliding core of 45 mm in diameter, rubber of 5 mm in thickness in each layer, and a shim plate of 2 mm in thickness. Three sliding plates were included in each layer, including two each with 1.5-mm acetyl or polyoxymethylene (POM) and one steel plate of 2 mm in thickness, to total 5 mm that was identical to the thickness of the rubber layer. These sliding plates were positioned between two adjacent shim plates to form two major sliding interfaces and were used to smooth the sliding motion of the sliding interfaces. As shown in Figs. 2 and 8, these arrangements are allowed two major sliding interfaces at each layer to slide during earthquakes. In these specimens used in this study, the contact surface between the shim and sliding plates did not become a sliding interface to protect the adhesive and rubber material. Therefore, the sliding displacement of each sliding interface was a half of the rubber deformation in each layer. The sliding plates were arranged in these experiments to achieve desired frictional force and avoid producing noise during sliding motion. More than two sliding interfaces in a single layer are possible and practical by using thinner sliding plates to further reduce displacement and heat at each sliding interface by adding sliding interfaces. Designing the contact surfaces between the shim and sliding plates as sliding interfaces for additional functionality may also be possible.

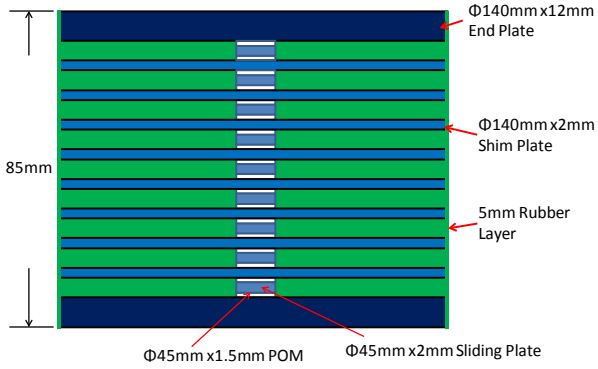

Fig. – 8 Details of the ARB Specimen

Fig. – 9 Internal view of a tested ARB specimen after more than 200 cycles of loadings

In general, the distributed sliding displacement of each sliding interface is much smaller than its diameter. The choice of materials for sliding plates depends on their vertical stiffness, high friction coefficient, strength, wear resistance, specific heat, and melting temperature. These are necessary to maintain functionality after the vulcanization and curing processes. The major reasons for combining steel and POM for use in sliding plates are that these materials are functional, remain silent during sliding motion, and are cheap and easy to acquire and manufacture. Still, other combinations of various materials are possible and practical.

Figure 9 shows an internal view of the ARB specimen after more than 200 cycle tests. This shows that no damage occurred to the tested ARB specimen even after a large number of cycling loadings and a high testing velocity of 176 mm/sec. It also reveals that the proposed rubber bearing is durable. Figures 10 and 11 show the hysteresis loops of the ARB specimen under a high vertical pressure of 13 MPa (130 kg/cm^2). Note that the shape factor of the bearing is as small as 4.75. For our experiment, we used a tested frequency of 0.7 Hz. Figures 10 and 11 show horizontal displacements of 20, and 40 mm, respectively. These figures demonstrate that the ARB seismic isolator possesses stable mechanical behavior. In addition, as we predicted in the mathematical formulations, the frictional force contributed by the sliding core (note the force at zero displacement) can, provide considerable damping to the isolator by viewing the enclosed area near the force-displacement loops. Moreover, the rubber material provides stiffness and little damping to the device, which yields smooth corners of the hysteresis loops without dramatic changes in stiffness.

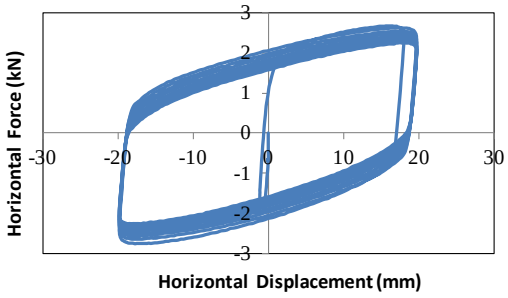

Fig. – 10 Hysteresis loop of ARB under 20 mm displacement and 0.7 Hz frequency

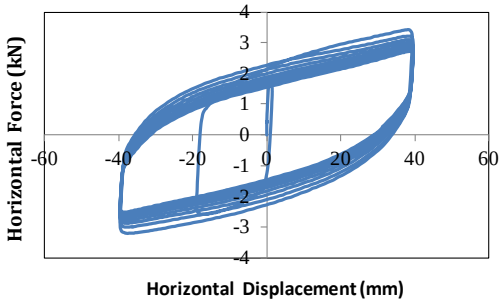

Fig. – 11 Hysteresis loop of ARB under 40 mm displacement and 0.7 Hz frequency

As Fig. 12 shows, the effective horizontal stiffness of the first cycle of the rubber bearing decreased with an increase in horizontal displacement as predicted in Eq. (28). In addition, the testing velocity had insignificant effects on the effective horizontal stiffness of the first cycle. The equivalent damping ratio decreased from 54.5% at a displacement of 5 mm to 43.0% at a displacement of 40 mm, as shown in Fig. 13, whereas the horizontal displacement increased. However, the equivalent damping ratio of the ARB remained extremely high at a large displacement compared to that with the LRB and high damping rubber bearing [5, 6]. Figure 13 also reveals that the equivalent damping ratio of the first cycle is insensitive to the testing frequency.

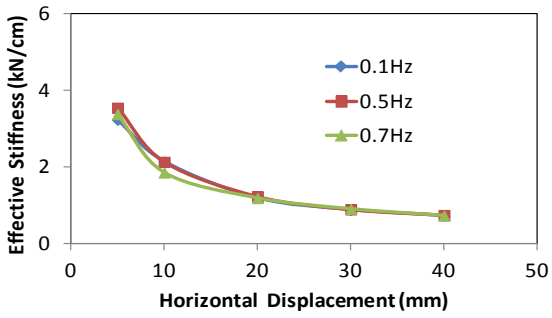

Fig. – 12 Effective stiffness of the first cycle of ARB under various tested displacements and frequencies

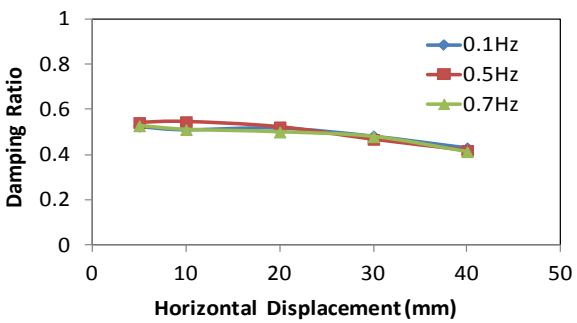

Fig. – 13 Damping ratio of the first cycle of ARB under various tested displacements and frequencies

Figures 14 and 15 illustrate the changes in effective stiffness and equivalent damping ratio, respectively, under several cycling loadings and various testing frequencies. These figures illustrate that effective stiffness and the equivalent damping ratio decreased when loading cycles increased because the increased accumulated energy resulted in temperatures rising, which weakened the material properties. In addition, the higher the testing frequency (i.e., the testing velocity), the greater was the influence on material properties. Therefore, the functionality and design of a rubber bearing for engineering practice should consider the effects of temperature rising during an earthquake. However, the temperature effect on the proposed ARB isolator, which showed a less than 6.5% change in the first three cycles, is much less when compared to the LRB, which showed approximately a 25% difference in the first three cycles [20]. The smaller percentage with the proposed ARB isolator occurred because the sliding mechanism in the sliding core of the ARB was uniformly distributed on all sliding surfaces between sliding plates.

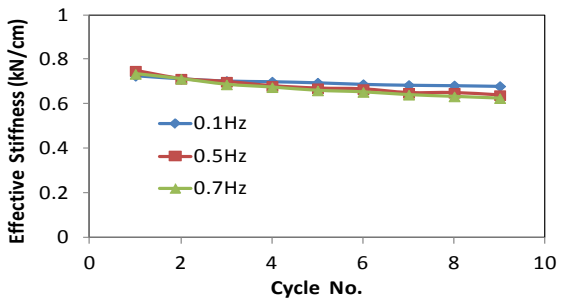

Fig. – 14 Effective stiffness of ARB under 40 mm displacement and various tested frequencies

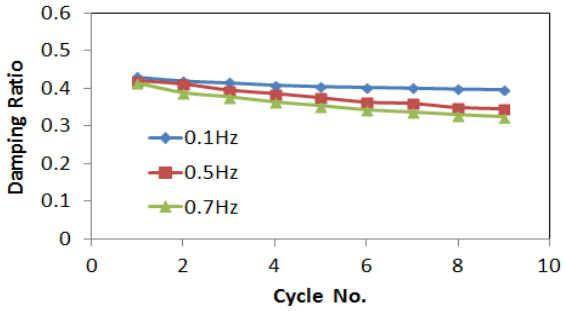

Fig. – 15 Damping ratio of ARB under 40 mm displacement and various tested frequencies

5. Conclusion

New seismic isolators known as ARBs were proposed in this study. The following conclusions can be drawn after theoretical and experimental investigations of the proposed devices:

1. The ARB isolator uses lead-free materials that are environment friendly.
2. The ARB isolator can sustain a high vertical pressure even with a small shape factor.
3. The ARB isolator possesses stable mechanical behavior.
4. The ARB isolator provides extremely high damping by means of a sliding mechanism in the sliding core. This mechanism consists of multiple sliding plates confined by two adjacent shim plates in each layer.
5. The decrease in equivalent damping ratio of the proposed devices that occurs with an increased displacement is not considerable even during high velocity cyclical loadings.
6. Rising temperature during an earthquake can have a reduced effect on the ARB isolator compared to that on the LRB.
7. The proposed rubber bearing is durable to sustain many reversal loadings.
8. The influence of accumulated energy on material properties under the first cyclic loading is insignificant because little energy is accumulated.
9. The greater the rate of accumulated energy, the greater is the change in material properties such as effective stiffness and equivalent damping ratio.

In summary, theoretical derivations and experimental results reveal that the proposed ARB is a promising seismic isolator that can be used to solve problems encountered in LRBs and HDRBs.

6. References

[1] Kelly JM (1986): Aseismic base isolation: review and bibliography. *Soil Dynamics and Earthquake Engineering*, **5**(4), 202-216.

[2] Buckle IG, Mayes RL (1990): Seismic isolation: history, application, and performance —A world view. *Earthquake Spectra*, **6**(2), 161-201.

[3] Tsai CS (2015): Seismic isolation devices: history and recent developments. In *the 2015 ASME Pressure Vessels and Piping Conference, Seismic Engineering*, Tsai, C. S. (ed.), Boston, MA, U. S. A., PVP2015-45068.

[4] Martelli A, Clemente P and Forni M (2015): Worldwide state-of-the-art of development and application of anti-seismic systems based on the information provided at the ASSISi Sendai Conference in 2013 and later and conditions for their correct use. *14th World Conference on Seismic Isolation, Energy Dissipation and Active Vibration Control of Structures*, San Diego, CA, U. S. A., on September 9-11.

[5] Kelly JM, Konstantinidis DA (2011): *Mechanics of Rubber Bearings for Seismic and Vibration Isolation*. John Wiley & Sons, Ltd.

[6] Tsai CS, Chiang TC, Chen BJ, Lin BS (2003): An advanced analytical model for high damping rubber bearings. *Earthquake Engineering and Structural Dynamics*, **32**, 1373-1387.

[7] Robinson WH (1978): *Cyclic Shear Energy Absorber*. US Patent No. 4117637.

[8] Zayas VA, Low SS, Mahin SA (1987): The FPS earthquake resisting system report. *EERC Technical Repor*t, UBC/EERC-87/01.

[9] Tsai CS, Chiang TC, Chen BJ (2003): Finite element formulations and theoretical study for variable curvature friction pendulum system. *Engineering Structures*, **25**(14), 1719-1730.

[10] Tsai CS, Chiang TC, Chen BJ (2003): Seismic behavior of MFPS isolated structure under near-fault sources and strong ground motions with long predominant periods. In *the 2003 ASME Pressure Vessels and Piping Conference, Seismic Engineering*, Chen, J. C. (ed.), Cleveland, Ohio, U. S. A., **466**, 73-79.

[11] Tsai CS, Chiang TC, Chen BJ (2003): Shaking table tests of a full scale steel structure isolated with MFPS. In t*he 2003 ASME Pressure Vessels and Piping Conference, Seismic Engineering*, Chen, J. C. (ed.), Cleveland, Ohio, U. S. A., **466**, 41-47.

[12] Tsai CS, Chen BJ, Pong WS, Chiang TC (2004): Interactive behavior of structures with multiple friction pendulum isolation system and unbounded foundations. *Advances in Structural Engineering, An International Journal*, **7**(6), 539-551.

[13] Tsai CS, Chiang TC and Chen BJ (2005): Experimental evaluation piecewise exact solution for predicting seismic responses of spherical sliding type isolated structures. *Earthquake Engineering and Structural Dynamics*, **34**(9), 1027–1046.

[14] Tsai CS, Lu PC, Chen WS, Chiang TC, Yang CT, Lin YC (2008): Finite element formulation and shaking table tests of direction-optimized friction pendulum system. *Engineering Structures*, **30**(9), 2321-2329.

[15] Fenz DM, Constantinou MC (2008): Spherical sliding isolation bearings with adaptive behavior-theory. *Earthquake Engineering and Structural Dynamics*, **37**(2), 168-183.

[16] Morgan TA, Mahin SA (2008): The optimization of multi-stage friction pendulum isolators for loss mitigation considering a range of seismic hazard. In *the 14th World Conference on Earthquake Engineering*, Beijing, China, Paper No. 11-0070.

[17] Sterne L (1869): *Improved Pneumatic Spring*. US Patent No. 87307.

[18] Tsai CS (2015): *Friction-Damping Energy Absorber*. Taiwan Patent No. M509823 and China Patent No. CN205013573U, Patents Pending in 15 Other Countries.

[19] Tsai CS, Su HC, Huang WC (2016): An Investigation of Adaptive Rubber Bearings. *ASME Pressure Vessels and Piping Conference, Seismic Engineering*, Vancouver, British Columbia, Canada, Paper No. PVP2016-63087.

[20] Benzoni G, Casarotti C (2008): Performance of lead-rubber and sliding bearings under different axial load and velocity conditions. *Report No. SRMD–2006/05-rev3*, Charles Lee Powell Structural Research Laboratories CalTrans SRMD Test Facility, Department of Structural Engineering University of California, San Diego La Jolla, CA, USA.